IJMT. Vol. 22, Iss. 2, 2026. (73-82)

International Journal of Maritime Technology

Journal homepage: ijmt.ir

# Numerical Investigation of Sea Wave and Oil Slick Interactions Using ANSYS AQWA Software

**Roshanak Khosrojerdi[1], Farhoud Kalate[2]**

[1] *PhD Student, Water and Hydraulic Structures, Faculty of Civil Engineering, University of Tehran, Tehran, Iran ; khosrojerdi.rosha@ut.ac.ir*

[2] *Associate Professor, Department of Water and Hydraulic Structures, Faculty of Civil Engineering, Tabriz University, Iran; fkalateh@tabrizu.ac.ir*

**ARTICLE INFO**

*Article History:*
Received: 4 Sep 2025
Last modification: 28 May 2026
Accepted: 30 May 2026
Available online: 30 May 2026

*Article type:*
Research paper

*Keywords:*
oil spill modeling,
wave-pollution interaction,
numerical simulation,
ANSYS AQWA,
marine pollution dynamics,
hydrodynamic analysis

**ABSTRACT**

Oil spills represent a critical source of marine pollution with profound environmental, economic, and social ramifications. This numerical study investigates the interaction between sea waves and oil slicks using ANSYS AQWA software to elucidate the dynamics of oil pollution distribution under wave action. The research examines three pollution mass models with varying dimensions under different wave approach angles (0°, 30°, and 60°) utilizing second-order Stokes wave theory. The investigation reveals that displacement of the pollution mass center decreases with increasing wave angle. Maximum displacement and mobility increase proportionally with expanding oil slick dimensions at constant mass. Wave-induced forces on pollution masses exhibit inverse correlation with wave angle. Forces from irregular waves exceed those from regular Stokes waves by approximately 20% for larger pollution masses. For expanded oil slicks, irregular wave forces can reach up to three times the magnitude of regular wave forces. These findings provide crucial insights for oil spill response planning, containment system design, and environmental impact assessment in marine environments.

ISSN: 2645-8136

**DOI:** http://dx.doi.org/10.66224/ijmt.22.2.73

**Copyright:** © 2026 by the authors. Submitted for possible open access publication under the terms and conditions of the Creative Commons Attribution (CC BY) license [https://creativecommons.org/licenses/by/4.0/]

[ Downloaded from ijmt.ir on 2026-09-13 ]

## 1. Introduction

Marine oil pollution constitutes one of the most persistent and devastating environmental challenges in contemporary oceanography, with profound environmental, economic, and social ramifications. The transport and dispersion mechanisms governing oil slicks in aquatic environments result from complex interactions among chemical, physical, and biological processes including advection, turbulent dispersion, evaporation, emulsification, dissolution, and biodegradation. Upon release onto the water surface, oil undergoes rapid initial spreading and forms a thin layer whose subsequent evolution is governed by external forcing from currents, wave action, and wind stress. The remote and inaccessible nature of maritime oil spill locations renders direct intervention economically prohibitive and logistically challenging, making numerical modeling an indispensable tool for predicting oil slick trajectories, estimating environmental impact, and optimizing cleanup strategies.

Modern oil spill modeling has evolved significantly since the early 2000s through sophisticated computational frameworks. Chao et al. [1] developed comprehensive 2D and 3D modeling systems investigating oil fate and transport processes, validated through a major fuel oil spill involving 28,500 tons in Singapore coastal waters. Operational capabilities advanced through Abascal et al. [2] TESEO system for real-time trajectory simulation and Chen et al. [3] Monte Carlo methodologies incorporating dynamic environmental conditions. Three-dimensional particle-based approaches were pioneered by Wang et al. [4] for comprehensive oil movement simulation, while Guo and Wang [5] developed hybrid Eulerian-Lagrangian methods combining hydrodynamic and wave modeling. Two-phase numerical modeling was advanced by Naghbi and Kolahdooz [6] and extended by Heydariha and Ghiassi [7] for regional applications. The practical significance of advanced modeling was demonstrated by Mariano et al. [8] during the Deepwater Horizon incident.

Contemporary research has significantly expanded oil spill modeling sophistication and wave interaction studies. Hou et al. [9] advanced containment system understanding through FLUENT simulations, revealing that wave action accelerates boom failure while opposing waves improve containment effectiveness. Feng et al. [10] developed three-dimensional VOF models for ship collision oil plume analysis, establishing critical relationships between plume behavior and collision parameters. Dąbrowska [11] enhanced regional-scale modeling through semi-Markov approaches for Baltic Sea predictions, demonstrating how environmental conditions drive slick fragmentation. Recent ANSYS platform applications include Putrananda et al. [12] and Nguyen et al. [13] utilizing ANSYS AQWA for vessel motion analysis, Arjomand et al. [14] demonstrating platform vibration control, Paiva et al. [15] optimizing wave energy converters with ANSYS-Fluent, and Wang et al. [16] examining environmental factor influences on wave characteristics.

Despite substantial advances, limited research has systematically investigated the parametric characteristics and effects of geometric and hydrodynamic factors on pollution distribution during wave interactions. Most existing models treat oil as particle collections focusing primarily on surface transport, with insufficient attention to fundamental wave-structure interaction mechanics. The specific influence of wave approach angles, scale effects of pollution mass dimensions, and comparative impacts of regular versus irregular wave conditions on oil slick dynamics remain inadequately understood.

This study addresses these fundamental questions through comprehensive computational fluid dynamics analysis using ANSYS AQWA software, investigating wave-oil slick interactions across multiple scales and wave conditions. The research examines three pollution mass models with varying dimensions under different wave approach angles (0°, 30°, and 60°) utilizing second-order Stokes wave theory. The investigation systematically evaluates wave approach angle influences on oil slick displacement patterns, scale effects on hydrodynamic response characteristics, regular versus irregular wave impact comparisons, and force characteristics related to pollution mass geometry. The findings reveal that displacement decreases with increasing wave angle, while mobility increases proportionally with expanding slick dimensions. Wave-induced forces exhibit inverse correlation with wave angle, with irregular wave forces exceeding regular wave forces by approximately 20% for larger masses, reaching up to three times the magnitude for expanded slicks. These results provide crucial insights for oil spill

[ Downloaded from ijmt.ir on 2026-09-13 ]

response planning, containment system design, and environmental impact assessment.

## 2. Materials and Methods

### 2.1 ANSYS AQWA Software Platform

ANSYS represents an advanced finite element simulation environment specifically designed for complex engineering analysis. The software foundation rests on sophisticated finite element methodologies capable of addressing diverse engineering challenges through comprehensive element libraries facilitating simulation of varied materials and structural configurations. A distinguishing characteristic of ANSYS is its superior capability for simulating different material models, setting it apart from other finite element software packages.

ANSYS AQWA specializes in hydrodynamic analysis of linear water wave loading on both fixed and floating structures. The software employs either wave diffraction theory or Morrison equations depending on the scale relationship between structure dimensions and wave characteristics. This section presents the theoretical foundation underlying boundary element analysis in ANSYS AQWA, including parameter extraction methods for hydrodynamic forces and effective parameters.

The modeling procedure involves several systematic steps: (1) wave motion modeling, (2) obstacle creation with specified contamination properties, (3) mesh generation and boundary condition definition, (4) solver application, and (5) output extraction. The interaction between oil slick and fluid is incorporated for enhanced modeling accuracy, with time-dependent boundary conditions accounting for dynamic wave effects.

### 2.2 Theoretical Foundation

### 2.2.1 Wave Force Analysis

Dynamic forces exerted on structures by waves are systematically categorized into three fundamental components:

- Pressure-induced dynamic forces
- Acceleration-induced dynamic forces
- Velocity-induced dynamic forces

For structures satisfying the condition $D/\lambda < 0.2$ (where D represents characteristic length and λ denotes wavelength), the structure cannot significantly influence incident wave characteristics. Under these conditions, pressure-induced dynamic force calculations proceed as follows:

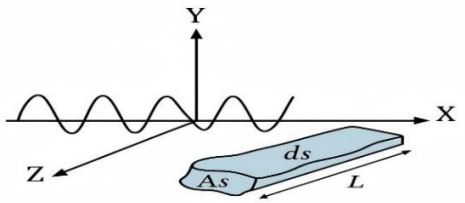


**Figure 1. Introduction of parameters used in calculations for dynamic force resulting from pressure**

$$PF = \iint_S -P_d \,.\, \vec{n}.\, ds \tag{1}$$

$$dF = P_d.\, ds \tag{2}$$

Where vector n represents a unit vector perpendicular to surface element ds and directed outward. Applying Green's theorem yields:

$$\iint_s -\mathrm{P_d}\,.\,\vec{\mathrm{n}}.\,\mathrm{ds} = \iiint_v -\vec{\nabla}\,.\,\mathrm{P_d}.\,\mathrm{dv} = \vec{\mathrm{i}}\iiint_v -\partial\mathrm{P}/_{\partial \mathrm{x}}\,.\,\mathrm{dx} + \vec{\mathrm{j}}\iiint_v -\partial\mathrm{P_d}/_{\partial \mathrm{y}}\,.\,\mathrm{dv} + \vec{\mathrm{k}}\iiint_v -\partial\mathrm{P}/_{\partial \mathrm{Z}}\,.\,\mathrm{dv} \tag{3}$$

Pressure calculations are performed at the center of the relevant structure. Dynamic forces resulting from acceleration and particle velocity are determined according to the following relationships:

[ Downloaded from ijmt.ir on 2026-09-13 ]

(a) (b)

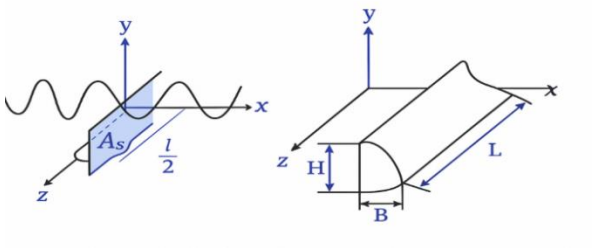


**Figure 2. Introduction of the parameters used in the calculations for dynamic force resulting from: a) acceleration and b) velocity**

$$FA_x = \int_{-1/2}^{1/2} (M_{AVM})_{HOR} \cdot a_x dz \quad (4)$$

$$FA_y = \int_{-1/2}^{1/2} (M_{AVM})_{VER} \cdot a_y dz \quad (5)$$

Where $(M_{AVM})_{HOR}$ represents the added mass coefficient of thin two-dimensional elements during horizontal oscillation, *and* $(M_{AVM})_{HOR}$ represents the corresponding coefficient for vertical oscillation.

Dynamic forces resulting from particle velocity (drag forces) are calculated as [17]:

$$F_{D,x} = {}^1\!/_2 \, pC_{D,x} \cdot \int_l Hdz.u|u| \quad (6)$$

$$F_{D,y} = {}^1\!/_2 \, pC_{D,y} \cdot \int_l Bdz.v|v| \quad (7)$$

## 2.4 Model Specifications and Computational Setup

This investigation analyzes three pollution mass configurations to systematically evaluate scale effects on wave-oil interactions:

**Table 1. Pollution Mass Model Specifications**

| Model Number | Dimensions (m) | Surface Area ($m^2$) | Volume ($m^3$) | Length-to-Thickness Ratio |
|---|---|---|---|---|
| Model 1 | 10 × 10 × 0.001 | 100 | 0.1 | 10,000 |
| Model 2 | 30 × 30 × 0.001 | 900 | 0.9 | 30,000 |
| Model 3 | 50 × 50 × 0.001 | 2,500 | 2.5 | 50,000 |

The computational investigation employed representative material properties with oil slick density set at 840 kg/m³ corresponding to medium crude oil characteristics, while seawater was modeled as a Newtonian, non-viscous fluid with density of 1025 kg/m³ under standard conditions at 15°C. Wave interactions were analyzed using second-order Stokes wave theory across three distinct approach angles (0°, 30°, and 60°) relative to pollution mass orientation, encompassing both regular and irregular sea state scenarios with variable frequency periods to systematically assess resonance effects on oil slick dynamics. The comprehensive computational analysis determined velocity profiles of pollution mass centers, spatial positioning evolution over time, and wave-induced force characteristics for each model configuration, with all results generated through ANSYS Workbench subsequently processed and analyzed using Excel software to enable detailed parametric evaluation of the hydrodynamic interactions between wave fields and oil pollution masses across multiple scales and environmental conditions.

## 2.5 Validation Methodology

To ensure computational accuracy and reliability, model validation was conducted through comparison with established experimental data from McGovern and Bai [19]. The validation focused on two critical aspects: maximum velocity estimation and acceleration prediction for floating plates under controlled wave conditions.

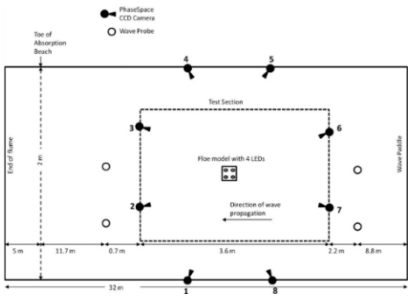


**Figure 3. Schematic representation of the experimental environment in McGovern's work[19]**

[ Downloaded from ijmt.ir on 2026-09-13 ]

To ensure computational accuracy and reliability, model validation was conducted through comparison with established experimental data from McGovern and Bai [19] using a wave flume environment with carefully controlled boundary conditions. The validation methodology employed a rectangular floating model with dimensions of 30 cm × 20 cm × 5 cm under specified wave parameters including a wave period of 1.389 seconds, wavelength of 290 centimeters, and wave height of 14.81 centimeters. This experimental configuration provided the necessary reference data for validating the computational model's capability to accurately predict maximum velocity estimation and acceleration characteristics for floating plates under controlled wave conditions, focusing on two critical aspects of oil slick motion dynamics that are essential for establishing confidence in the numerical simulation results generated by the ANSYS AQWA framework.

**Table 2. Validation Parameters**

| Parameter | Value | Units |
|---|---|---|
| Wave Period (T) | 1.389 | seconds |
| Wavelength (λ) | 290 | centimeters |
| Wave Height (H) | 14.81 | centimeters |
| Model Length | 30 | centimeters |
| Model Width | 20 | centimeters |
| Model Thickness | 5 | centimeters |

## 3. Results and Discussion

### 3.1 Model Validation Results

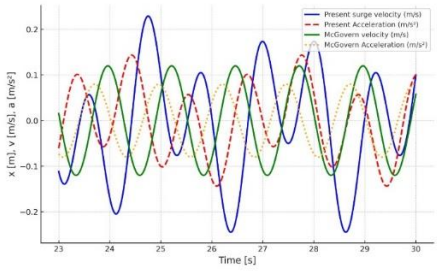


**Figure 4. Validation of the maximum velocity and acceleration of the center of the floating plate surface**

The validation analysis demonstrates satisfactory agreement between computational predictions and experimental observations. Maximum surge velocity (VX = 0.3 m/s) occurs approximately at the midpoint between trough and crest displacement cycles, corresponding to a surge velocity ratio VP = 0.82 relative to theoretical particle velocity calculations. Maximum instantaneous acceleration (AX = 12.0 m/s²) occurs when velocity approaches zero, consistent with fundamental wave dynamics theory. This validation confirms the computational model's capability to accurately predict oil slick motion characteristics under controlled wave conditions.

### 3.2 Angular Effects Analysis: Wave Approach Angle Impact (θ: 0° to 60°)

The systematic investigation of wave approach angle effects represents the core contribution of this research, revealing fundamental relationships governing wave-oil slick interactions across different scales.

#### 3.2.1 Scale-Dependent Displacement Response

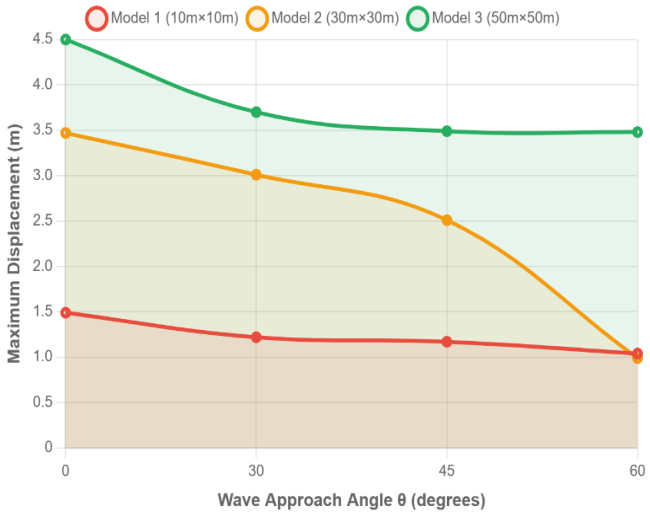


**Figure 5. Maximum Displacement vs Wave Approach Angle**

Figure 5 demonstrates the systematic decrease in maximum oil slick displacement as wave approach angle increases from 0° to 60° across all three model configurations. The results reveal distinct scale-dependent angular sensitivity patterns governed by wave-structure interaction physics. Model 2 (30m×30m) exhibits an exceptional 71% displacement reduction due to critical dimension resonance occurring



[ Downloaded from ijmt.ir on 2026-09-13 ]

at D/λ = 0.10, where the slick operates in the optimal diffraction regime for maximum wave-structure coupling. The 30m dimension matches the characteristic horizontal orbital diameter of surface wave particles (≈ λ/10 for second-order Stokes waves), creating maximum momentum coupling that varies as cos²(θ). In contrast, Model 1 (10m×10m) shows gradual reduction (30%) due to minimal wave interaction at D/λ = 0.033, while Model 3 (50m×50m) exhibits moderate reduction (23%) because inertial effects dominate at D/λ = 0.167, creating system damping that reduces angular sensitivity.

### 3.2.2 Normalized Angular Sensitivity Analysis

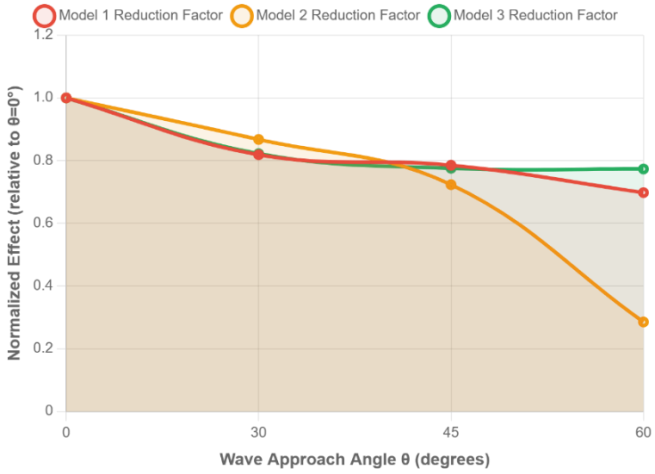


**Figure 6. Angular Effect Reduction Factor Analysis**

Figure 6 presents the normalized reduction factors that isolate angular sensitivity effects from absolute magnitude differences, revealing underlying wave-structure interaction physics. The normalization η = Displacement(θ)/Displacement(0°) exposes fundamental angular transfer functions. Model 2's extreme sensitivity (η = 0.29 at 60°) results from resonance-enhanced angular dependency, where the resonance amplification factor $A(\theta) = [1 + R_0 \cos^2(\theta)]^{-1}$ with $R_0 \approx 3.5$ for the critical dimension ratio. The analysis reveals a universal critical angle around θ = 30° where interaction characteristics shift from wave-following (0°-30°) to wave-crossing dynamics (30°-60°), with the transition governed by boundary layer physics and orbital motion alignment.

### 3.2.3 Hydrodynamic Force Scaling

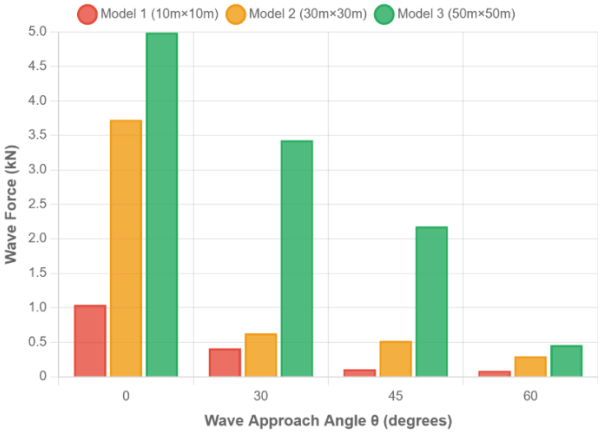


**Figure 7. Wave Force Analysis Under Angular Variations**

Figure 7 demonstrates systematic force reduction following $F = F_0 \cos^2(\theta) \times S(D/\lambda)$, where $S(D/\lambda)$ represents scale-dependent force amplification. The quadratic angular dependency arises from coupled geometric projection ($A_{eff} = A_0 \cos(\theta)$) and dynamic pressure scaling ($p_{dyn} \propto \cos(\theta)$). Model 3 experiences maximum absolute forces (4.99 kN at 0°) due to inertial scaling $F \propto \rho A D^2 \omega^2$, while Model 2 shows elevated force levels (3.73 kN at 0°) enhanced by diffraction effects at the critical dimension ratio. The consistent 90%+ force reduction across all scales confirms the fundamental cos²(θ) dependency and provides quantitative design criteria for containment systems: $F_{design} = F_0 \cos^2(\theta_{max}) \times S(D_{spill}/\lambda_{design})$

### 3.2.4 Velocity Response of Oil Pollution Models Under Various Wave Approach Angles

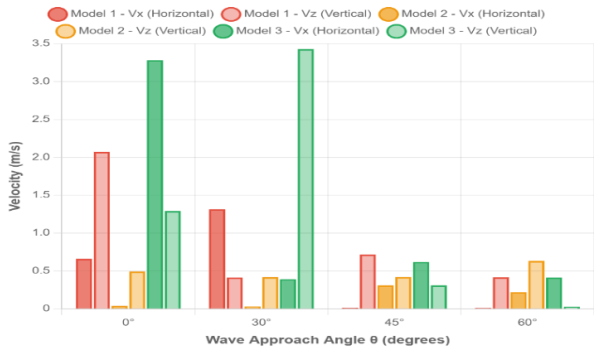


**Figure 8. Maximum velocity components (horizontal Vx and vertical Vz) for three oil sheet models under different wave approach angles**

[ Downloaded from ijmt.ir on 2026-09-13 ]

The velocity response characteristics of the three oil pollution models demonstrate significant variations based on both the oil sheet dimensions and wave approach angles, as illustrated in Figure 8. Model 3, representing the largest oil sheet (50×50×0.001 m), exhibits the highest velocity magnitudes in both horizontal and vertical directions, with maximum vertical velocities reaching approximately 3.4 m/s at 0° wave approach angle. This enhanced response can be attributed to the increased surface area interaction with wave forces, resulting in greater hydrodynamic coupling. Conversely, the smallest model (Model 1: 10×10×0.001 m) shows the most moderate velocity responses, with maximum horizontal velocities around 0.7 m/s and vertical velocities reaching 2.0 m/s under direct wave incidence. A consistent trend across all models indicates that velocity magnitudes decrease substantially as the wave approach angle increases from 0° to 60°, with the most pronounced reduction occurring in the vertical velocity component. This angular dependency reflects the reduced effective wave energy transfer to the oil sheet as the wave direction deviates from normal incidence, demonstrating the critical role of wave directionality in oil spill transport dynamics.

### 3.3 Comprehensive Parametric Analysis Results

**Table 3. Hydrodynamic Analysis Results Summary (T = 1.389s)**

| Model | Wave Angle | Force (kN) | Max Position (m) | Vx (m/s) | Vz (m/s) | Force Ratio |
|---|---|---|---|---|---|---|
| 1 | 0° | 1.044 | 1.490 | 0.661 | 2.072 | 1.00 |
| 1 | 30° | 0.413 | 1.224 | 1.316 | 0.413 | 0.40 |
| 1 | 45° | 0.106 | 1.170 | 0.016 | 0.717 | 0.10 |
| 1 | 60° | 0.085 | 1.044 | 0.012 | 0.416 | 0.08 |
| 2 | 0° | 3.726 | 3.470 | 0.712 | 3.346 | 1.00 |
| 2 | 30° | 0.629 | 3.010 | 0.970 | 0.958 | 0.17 |
| 2 | 45° | 0.520 | 2.513 | 0.310 | 0.419 | 0.14 |
| 2 | 60° | 0.296 | 0.987 | 0.220 | 0.633 | 0.08 |
| 3 | 0° | 4.991 | 4.500 | 3.281 | 1.293 | 1.00 |
| 3 | 30° | 3.429 | 3.700 | 0.390 | 3.371 | 0.69 |
| 3 | 45° | 2.180 | 3.490 | 0.620 | 0.310 | 0.44 |
| 3 | 60° | 0.459 | 3.480 | 0.345 | 0.027 | 0.09 |

### 3.4 Scale Effects and Force Scaling

The investigation reveals systematic relationships between pollution mass scale and hydrodynamic response characteristics:

- Displacement Scaling: Maximum displacement in the surge direction increases proportionally with pollution mass spread, indicating enhanced mobility for larger spills under identical wave conditions.
- Velocity Relationships: Vertical velocity components (Vz) consistently exceed horizontal components (Vx) across all model scales, suggesting predominant heave motion characteristics. This finding indicates that vertical mixing processes may be more significant than horizontal transport for oil-water interaction.
- Force Amplification: Maximum force values increase systematically with pollution mass spread. This relationship follows expected theoretical predictions based on increased wetted surface area and enhanced wave-structure interaction.

### 3.6 Frequency Response Characteristics

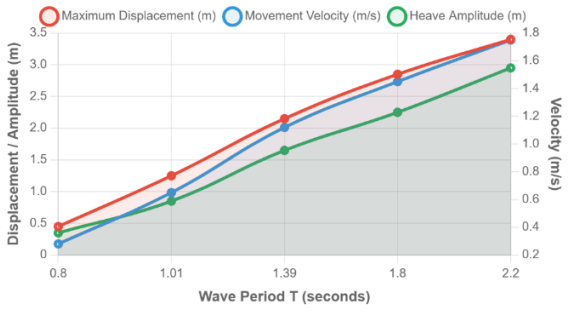


**Figure 9. Wave period effects on oil slick movement velocity and displacement characteristics**



[ Downloaded from ijmt.ir on 2026-09-13 ]

Investigation of frequency response characteristics reveals complex relationships between wave period and oil slick dynamics:

- Velocity Correlation: Oil slick movement velocity increases proportionally with wave period, indicating enhanced transport potential for longer-period waves.
- Heave Amplitude: Increasing wave period results in enhanced heave amplitude (z-direction movement), suggesting increased vertical mixing potential.
- Frequency Dependency: At intermediate frequencies, heave amplitude variations do not follow consistent trends with velocity increases, indicating complex resonance effects.
- Angular Effects: Transitioning from 0° to 60° wave approach angles produces variable heave amplitude responses, with both increases and decreases observed depending on specific frequency conditions.

### 3.7 Environmental and Practical Implications

The research findings provide several important insights for marine pollution management:

Spill Response Planning: Understanding angular dependency of oil transport enables improved prediction of pollution trajectories under varying wave approach conditions. This knowledge can optimize containment boom placement and recovery vessel positioning.

Containment System Design: Force scaling relationships with pollution mass dimensions inform structural design requirements for containment systems, particularly under irregular sea state conditions where forces can be substantially amplified.

Environmental Impact Assessment: The dominance of vertical velocity components suggests that oil-water mixing processes may be more significant than previously assumed in environmental impact calculations.

Operational Considerations: The substantial differences between regular and irregular wave effects indicate that operational planning based solely on regular wave analysis may significantly underestimate force requirements and system loading.

## 4. Limitations and Future Work

This study focuses on idealized pollution mass geometries under controlled wave conditions. Future investigations should consider:

- Realistic Oil Properties: Investigation of time-dependent oil properties including viscosity changes, emulsification effects, and weathering processes
- Complex Geometries: Analysis of irregular pollution mass shapes and fragmented slick configurations
- Multi-Physics Coupling: Integration of wind effects, current interactions, and temperature variations
- Field Validation: Comparison with real spill event data to validate model predictions under operational conditions

## 5. Conclusions

This numerical investigation of wave-oil slick interactions using ANSYS AQWA provides critical insights for understanding marine pollution dynamics and developing effective response strategies. The research demonstrates that wave approach angle significantly influences pollution transport characteristics, with displacement decreasing systematically as incident angle increases from normal incidence, providing a foundation for predicting oil movement under varying wave directional conditions. Larger oil slicks experience enhanced displacement and force loading while maintaining constant mass, indicating increased mobility potential for major spill events with important implications for response time requirements and containment strategy development. Notably, vertical motion components consistently dominate horizontal transport across all scales and conditions, suggesting that heave dynamics play a crucial role in oil-water mixing processes and should be prioritized in environmental impact assessments. Wave-induced forces scale positively with pollution surface area, providing quantitative relationships for predicting containment system loading requirements and structural design specifications. These findings

[ Downloaded from ijmt.ir on 2026-09-13 ]

contribute to several practical applications in marine environmental management, including enhanced spill trajectory prediction through improved understanding of angular effects for more accurate response planning, informed containment system design where force scaling relationships guide structural requirements for booms and barriers under realistic sea conditions, optimized response strategies where scale effects inform deployment approaches for different spill magnitudes, and improved environmental impact assessment where motion characteristics provide better estimates of mixing and dispersion processes in marine environments.

## 6. Author Contribution

Roshanak Khosrojerdi conceptualized and designed the study, developed the methodology, conducted all data collection and formal analysis, performed data curation and visualization, wrote the original draft, and revised the manuscript. Roshanak Khosrojerdi also serves as the corresponding author. Farhoud Kalate contributed to the initial conceptualization by suggesting the research topic and providing relevant literature recommendations. Roshanak Khosrojerdi conducted all other aspects of the research independently. Both authors have read and approved the final version of the manuscript.

## 7. Data Availability Statement

The datasets generated and analyzed during the current study are available from the corresponding author upon reasonable request. Due to privacy and ethical considerations, raw data cannot be shared publicly. However, aggregated data supporting the conclusions of this article are included within the manuscript and its supplementary information files. Researchers interested in accessing the underlying data for replication or further analysis may contact the corresponding author to discuss data sharing arrangements in accordance with institutional review board guidelines and applicable data protection regulations.

## 8. References


1- Chao, X., Shankar, N.J., & Cheong, H.F. (2001). *Two-and three-dimensional oil spill model for coastal waters*. Ocean Engineering, Vol.28(12),p.1557-1573, https://doi.org/10.1016/S0029-8018(01)00025-X.

2- Abascal, A.J., Castanedo, S., Gutierrez, A.D., Comerma, E., Medina, R., & Losada, I.J. (2007). *TESEO: An operational system for simulating oil spill trajectories and fate processes.* ISOPE International Ocean and Polar Engineering Conference , p. 1916-1923, https://doi.org/10.17632/vby7m2p42w.1.

3- Chen, H.Z., Li, D.M., & Li, X. (2007). *Mathematical modeling of oil spill on the sea and application of the modeling in Daya Bay.* Journal of Hydrodynamics , Vol. 19(3), p. 282-291,https://doi.org/10.1016/S10016058(07)60060-3.

4- Wang, S.D., Shen, Y.M., Guo, Y.K., & Tang, J. (2008).*Three-dimensional numerical simulation for transport of oil spills in seas.* Ocean Engineering , Vol. 35(5-6), p. 503-510, https://doi.org/10.1016/j.oceaneng.2007.12.001.

5- Guo, W.J., & Wang, Y.X. (2009). *A numerical oil spill model based on a hybrid method.* Marine Pollution Bulletin , Vol. 58(5), p. 726-734,https://doi.org/10.1016/j.marpolbul.2008.12.012., 58(5), 726-734.

6- Nagheeby, M., & Kolahdoozan, M. (2010). *Numerical modeling of two-phase fluid flow and oil slick transport in estuarine water.* International Journal of Environmental Science &Technology,Vol.7(4),p.771-784, https://doi.org/10.1007/BF03326186.,7,771-784.

7- Heydariha, J.Z., & Ghiassi, R. (2010*). Oil spill simulation in the mouth of the Persian Gulf.* Advances in Waste Management , Vol. 1(2), p. 56-60,https://doi.org/10.5281/zenodo.1082143.

8- Mariano, A., et al. (2011). *On the modeling of the 2010 Gulf of Mexico oil spill.* Dynamics of Atmospheres and Oceans , Vol. 52(1-2), p. 322-340,https://doi.org/10.1016/j.dynatmoce.2011.06.001.

9- Hou, T., Sun, H., Jiao, B., Wang, G., Lin, H., Liu, H., & Gao, B. (2024). *Numerical and experimental study of oil boom motion response*




[ Downloaded from ijmt.ir on 2026-09-13 ]

*and oil-stopping effect under wave-current action*. Ocean Engineering ,Vol. 291, p. 116439,https://doi.org/10.1016/j.oceaneng.2023.116439.

10- Feng, X., Liu, Y., Wei, Q., Su, J., Zhang, D., Zhou, Z., Wu, W., Xiong, C., & Peng, S. (2024). *Numerical simulations on the oil plume evolutions and the two critical aspects of emergent oil containment for ship collision-incurred oil spills*. Ocean Engineering Vol. 305, p.118030,https://doi.org/10.1016/j.oceaneng.2024.118030.

11- Dąbrowska, E. (2024). *Numerical Modelling and Prediction of Oil Slick Dispersion and Horizontal Movement at Bornholm Basin in Baltic Sea*. Water , Vol. 16(8), p. 1088, https://doi.org/10.3390/w16081088.

12- Putrananda, M.B.S., Bahatmaka, A., Aryadi, W., Puteri, B.A., & Hutagalung, C.I. (2025). *Numerical Analysis of Six Degrees of Freedom Motion Response of Trimaran Semi-Submersible Ship*. Mekanika: Majalah Ilmiah Mekanika,Vol.24(1),p.61-72, https://doi.org/10.20961/mekanika.v24i1.82103.

13- Nguyen, T.T., Phan, T.L., & Le, T.H. (2025). *Numerical Study on the Motion and Wave Loads of an Uncrewed Surface Vehicle Catamaran at Low Speed in Sea Waves*. Journal of Applied Fluid Mechanics , Vol. 18(9), p. 2321-2331, https://doi.org/10.47176/jafm.18.09.2831*.,* 18(9), 2321-2331.

14- Arjomand, M.A., Bagheri, M., & Mostafaei, Y. (2025). *Performance Enhancement of Tuned Liquid Dampers in Fixed Offshore Platforms: A Coupled ANSYS Aqwa-Transient Structural Approach*.Civil Engineering and Applied Solutions,Vol.1(1),p.77-88, https://doi.org/10.61186/ceas.1.1.77.

15- Paiva, M.S., Mocellin, A.P.G., Oleinik, P.H., Santos, E.D., Rocha, L.A.O., Isoldi, L.A., & Machado, B.N. (2025*). Geometrical Evaluation of an Overtopping Wave Energy Converter Device Subject to Realistic Irregular Waves and Representative Regular Waves of the Sea State That Occurred in Rio Grande-RS*. Processes*,* Vol.13(2),p.335,https://doi.org/10.3390/pr13020335.

16- Wang, P., Yu, W., Zhao, M., & Du, X. (2024). *Effects of wind-wave-current-earthquake interaction on the wave height and hydrodynamic pressure based on CFD method* ,Ocean-Engineering,Vol.305,p.117909,https://doi.org/10.1016/j.oceaneng.2024.117909.

17- Constantin, A. (2016). *Extrema of the dynamic pressure in an irrotational regular wave train. Physics of Fluids* , Vol. 28(11), p. 113604, https://doi.org/10.1063/1.4967831.

18- Chakrabarti, S. (2005*). Handbook of Offshore Engineering* (2-volume set) , Elsevier, ISBN: 978-0080443812,https://doi.org/10.1016/B978-0-08-044381-2.X5000-5.

19- McGovern, D.J., & Bai, W. (2014). *Experimental study on kinematics of sea ice floes in regular waves*. Cold Regions Science and Technology ,Vol. 103, p.124-130, https://doi.org/10.1016/j.coldregions.2014.03.007.

[ Downloaded from ijmt.ir on 2026-09-13 ]